Food Chemistry 112 (2009) 267–272

Contents lists available at ScienceDirect

Food Chemistry

journal homepage: www.elsevier.com/locate/foodchem

Analytical Methods

Artifacts in the measurement of water distribution in soybeans using MR imaging

Young-Shick Hong [a], Jee-Hyun Cho [b], Na-Ri Kim [a], Chulhyun Lee [b], Chaejoon Cheong [b], Kwan Soo Hong [b], Cherl-Ho Lee [a,*]

[a] School of Life Science and Biotechnology, Korea University, Seoul 136-701, Republic of Korea
[b] MRI Team, Korea Basic Science Institute, Cheongwon 363-883, Republic of Korea

ARTICLE INFO

Article history:
Received 29 December 2007
Received in revised form 22 April 2008
Accepted 26 May 2008

Keywords:
T_1-weighted
T_2^*-weighted
T_2-weighted
Magnetic resonance (MR) images
Chemical shift selective MR images
Lipid suppression
Water suppression
Soybean

ABSTRACT

Significant artifacts occur from the overlapping signals of the water and lipids in relaxation time-weighted magnetic resonance (MR) images and should be compensated, in order to determine a precise water distribution in the soybean seeds. The chemical shift selective T_1-, T_2^*-, and T_2-weighted MR images of water were compared to those with water or lipid suppression in soaked soybean seeds. In the absence of lipid suppression, the chemical shift artifacts were observed in the chemical shift selective T_1- and T_2-weighted MR images, due to the overlapping signals of the water and lipid protons. However, the MR images with lipid suppression had reduced artifacts. This study demonstrates that an appropriate MR imaging technique provides relatively uniform signal intensity and has importance in the investigation of true water distribution within food systems, such as to correlate a relationship between water distribution using MR imaging and water diffusion using pulsed field gradient (PFG) NMR.

1. Introduction

Soybeans accumulate large amounts of lipid and protein, accounting for significant portions within the global food and feed supply; in Asia especially, soybeans are a major protein sources, where various traditional foods such as soybean curd and fermented soybean products are produced (Lee, 2001).

Water plays a critical role in the chemical and enzymatic reactions as well as the thermal treatment of soybeans, resulting in protein denaturation and polysaccharide gelatinization. Moisture transfer is therefore a governing factor of soybean processing. Mass transfer analyses of food systems are difficult due to their complex and heterogeneous nature. For example, microstructural features such as the coat, micropyle, and hilum, as well as composition of the seed coat in soybean seeds, may affect the imbibition rate (Agbo, Hosfield, Uebersax, & Klomparens, 1987; Deshpande & Cheryan, 1986; Marbach & Mayer, 1974). The theoretical models of water diffusion have assumed that the bean coat, for resisting water sorption, is gradually increased by surface moisture (Vertucci, 1989), and Schwartzberg and Chao have reviewed the mathematics of mass transport processes in food materials (Schwartzberg & Chao, 1983). Most of the studies on water uptake by seeds are destructive in nature, thus non-invasive and non-destructive methods are required. Magnetic resonance (MR) imaging is the most appropriate technique for this purpose. With the recent development of high-field NMR spectrometers capable of MR imaging, the sensitivity and resolution of MR imaging have increased dramatically, showing a quick and reliable means to non-invasively access the internal structures of plants, fruits, and processed foods, and to study water distribution. MR imaging was successfully applied to investigate water uptake and distribution in soybean seeds (Pietrzak, Fregeau-Reid, Chatson, & Blackwell, 2002), developing barely grains (Glidewell, 2006), western white pine seeds (Terskikh, Feurtado, Ren, Abrams, & Kermode, 2005), germinating tobacco seeds (Manz, Muller, Kucera, Volke, & Leubner-Metzger, 2005), the coating of tempura (Horigane, Motoi, Irie, & Yoshida, 2003), cooked spaghetti (Irie, Horigane, Naito, Motoi, & Yoshida, 2004), and cooked rice kernels (Mohoric et al., 2004).

High-resolution MR imaging could be very useful for examining the structural features of seeds, and for detailed analysis of the process of imbibition and cooking. In this study, the MR images of soaked soybean seeds were acquired with various MR imaging sequences, and the best imaging methods were suggested for investigating the true water distribution in soaked and cooked soybean seeds, compensating for the artifacts of the images.

* Corresponding author. Tel.: +82 2 3290 3414; fax: +82 2 927 5201.
E-mail address: chlee@korea.ac.kr (C.-H. Lee).

0308-8146/$ - see front matter © 2008 Elsevier Ltd. All rights reserved.
doi:10.1016/j.foodchem.2008.05.109

2. Materials and methods

2.1. Materials

Soybean seeds (*Glycine max*) harvested in Korea in 2005 were used for this study. For the soaking experiment, 3 g soybean seeds were immersed in water for 1, 4, and 15 h at 37 °C. And for the cooking experiment, 3 g soybean seeds were soaked for 15 h and boiled in 30 g of distilled water in triangle glass flasks for 5, 30, 60, and 120 min, separately. Moisture, lipid, and protein contents were determined in dried soybean seeds using the standard AOAC methods (AOAC, 1990): lipids, 17.88% (±0.37); water content, 6.12% (±0.05); protein, 39.17% (±0.42); ash, 4.89% (±0.13). For the MR images, peanut seeds (*Arachis hypogaea*) were also soaked for 15 hours and compared with the MR images of the soybean seeds.

2.2. MR imaging and NMR spectroscopy

The soybean seed was inserted into an NMR tube with an outside diameter of 10 mm, and fixed with three pieces of acrylic plate (4 mm × 16 mm) to prevent moving induced by the gradient coil. The MR imaging experiments were performed on a 14.1 Tesla NMR spectrometer (Bruker Avance DMX600SB) equipped with a standard micro imaging accessory. For acquisition and processing of the NMR data, the Paravision and Xwin-NMR programs (Bruker) were used. Spin-lattice relaxation (T_1)-weighted, susceptibility (T_2^*)-weighted and spin-spin relaxation (T_2)-weighted MR images were acquired using the multi-slice multi-echo (MSME), gradient echo fast imaging (GEFI), and rapid acquisition with relaxation enhancement (RARE) sequences, respectively. The chemical shift selective method was applied to all the MR images to acquire water and lipid images simultaneously. The bandwidths for the water or lipid suppression were 4000 Hz and 2000 Hz at 4.8 ppm and 1.3 ppm, respectively. The repetition time (T_R) and echo time (T_E) were 1 s and 7.4 ms for MSME, respectively. The T_R/T_E were 1 s/4.3 ms for GEFI and 5 s/35.0 ms for RARE. The central slice of 10 multi-slices is shown in the coronal plane of the MR images in the Results. In all experiments, the field of view (FOV) was 0.7 cm × 0.7 cm, and the slice thickness was 1.0 mm. The matrix size was 256 × 256 for all the MR images, resulting in 27 × 27 μm^2 of in-plane resolution.

^{1}H static NMR spectra were recorded with the same MR imaging probe applying a simple single-pulse sequence. The pulse length of ^{1}H $\pi/2$ was 22.8 μs. Typically, 16 scans were accumulated with a 22.8 μs pulse and a recycle delay of 5 s. For magic angle spinning (MAS) NMR spectroscopy, the dried soybeans were ground by a grinder and the spectrum was acquired in a standard 4-mm o.d. MAS rotor, using a Bruker Avance 400 MHz ^{1}H NMR spectrometer with a spinning rate of 1 kHz.

3. Results and discussion

3.1. Static and MAS NMR spectroscopy

The soybean seeds (3 g) absorbed 2.74 g (±0.13) of water in 15 h of soaking time while amount of absorbed water was 0.71 g (±0.30) in 1 h. The representative ^{1}H NMR spectra obtained from the soybean seeds soaked in water for 15 hours are shown in Fig. 1. Fig. 1A is a static 600 MHz ^{1}H NMR spectrum, and the two broad peaks were assigned to the water and lipids. Fig. 1B is a magic angle spinning (MAS) 400 MHz ^{1}H NMR spectrum of the ground soybeans. The lipids were further assigned mainly as triacylglycerols, glycerolipids, and phospholipids using the magic angle spinning (MAS) NMR. These lipid signals acquired by NMR spectroscopy were also found by other investigators for mature soybean seeds (Borisjuk et al., 2005), western white pine seeds (Terskikh et al., 2005), tobacco seeds (Manz et al., 2005) and barley kernels (Gruwel, Chatson, Yin, & Abrams, 2001).

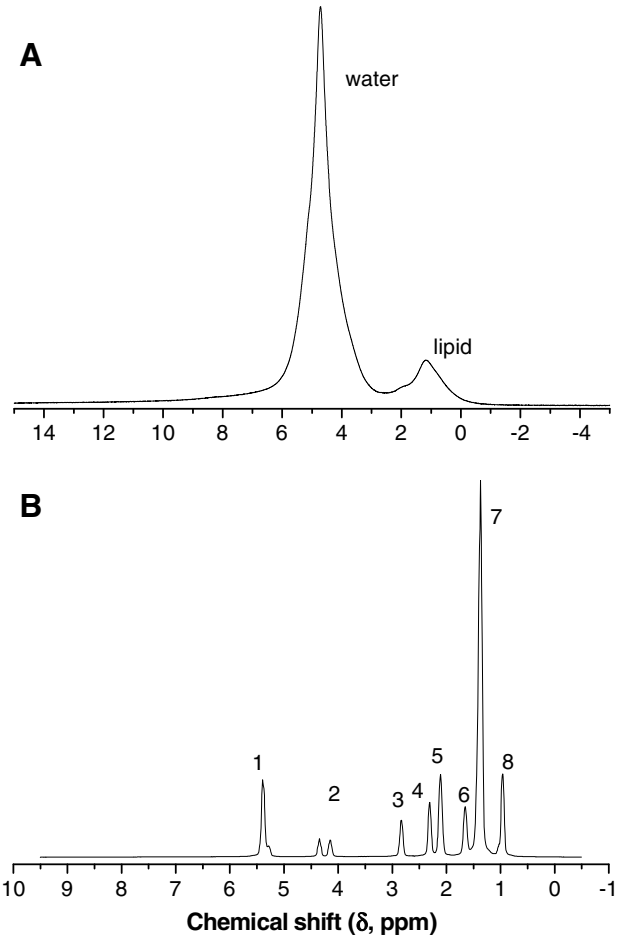

Fig. 1. A static 600 MHz ^{1}H NMR spectrum for soaked soybean seed (A) and a MAS NMR spectrum of ground soybeans (B). 1, –C***H***=C***H***–; 2, glycerol backbone; 3, –**CH**=CH–C***H***$_2$–CH=CH–; 4, –C***H***$_2$–CH$_2$–; 5, (CH$_2$)$_n$–C***H***$_2$–CH=CH; 6, –CH$_2$–C***H***$_2$–; 7, –CH$_2$–(C***H***$_2$)$_6$–CH$_3$ and 8, (CH$_2$)$_n$–C***H***$_3$. Italic **bold** type signifies proton resonance observed.

3.2. Relaxation time-weighted MR images

Fig. 2A–C show the chemical shift selective T_1-weighted, T_2^*-weighted, and T_2-weighted MR images, using the MSME (multi-slice multi-echo), GEFI (gradient echo fast imaging), and RARE (rapid acquisition with relaxation enhancement) sequences, respectively. The chemical shift of water was chosen in order to exclude the effect of lipid in the MR images, because the soybeans contained 17.88% (w/w) lipid. The highest signal intensity was found in the void between the cotyledons, due to the bulk water within the void. Vascular bundles (VB) were obviously found in the T_2^*-weighted MR image, and this image provides a greater difference in contrast, as compared to the T_1- and T_2-weighted MR images. This effect was clear when the images were expressed in gray scale, as shown in Fig. 2G–L.

In general, the signals of the ^{1}H magnetic resonance (MR) images originate from the water and lipids. A strong signal for water is observed in the soaked soybean seeds, as well as the lipid signal. Accordingly, the structural details are not very clear. In such cases, contrast based on the differences in proton mobility is useful. The mobility of proton molecules is related to the spin-lattice relaxation time (T_1) and the spin-spin relaxation time (T_2). The

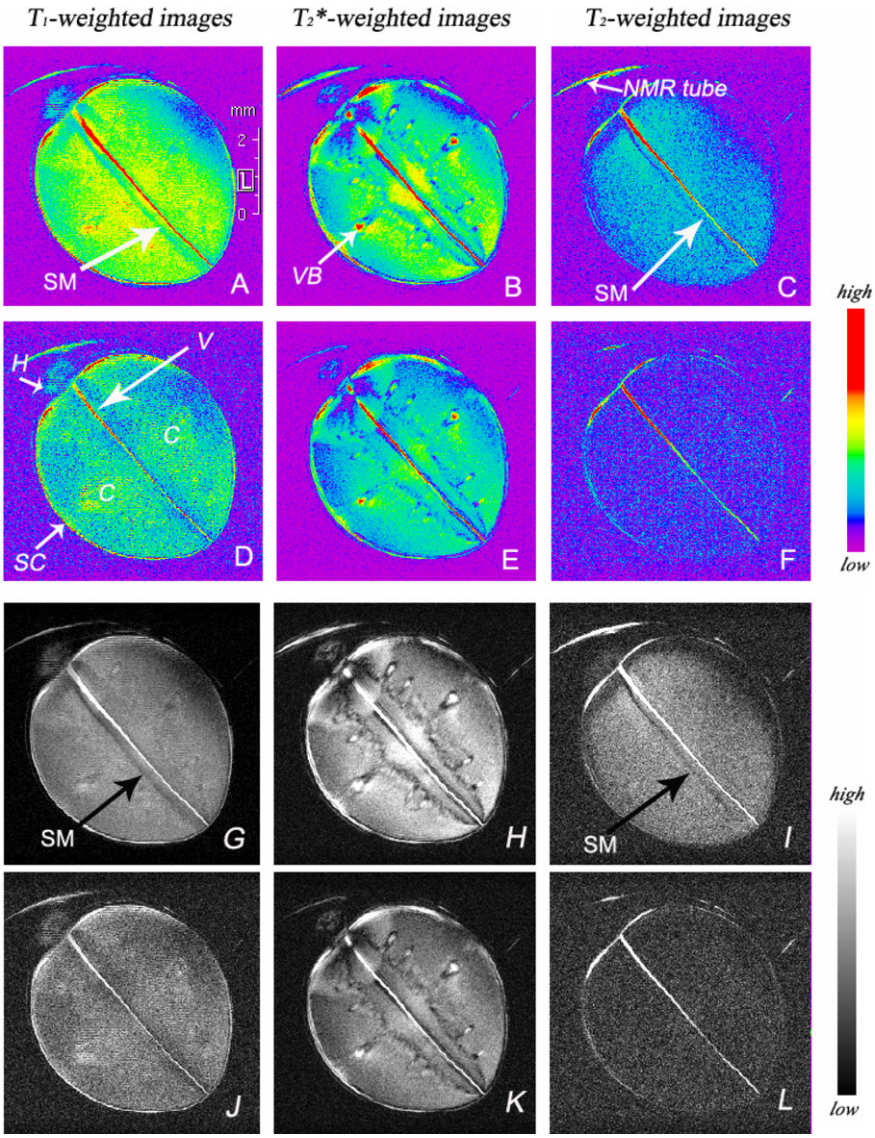

Fig. 2. Chemical shift selective MR images of water in soybeans soaked in water for 15 hrs using various spin-echo sequences. A, B, and C are chemical shift selective T_1-, T_2^*-, and T_2-weighted MR images, respectively, without lipid suppression. D, E, and F are chemical shift selective T_1-, T_2^*-, and T_2-weighted MR images, respectively, with lipid suppression. All images show central slices in the axial plane. The MR images were obtained with $27 \times 27\ \mu m^2$ in-plane resolution and a 1 mm slice thickness. H, hillum; C, cotyledons; VB, vascular bundles; SC, seed coat; V, void between cotyledons and SM, shadow misregistration. G–L are the same MR images as A–F except they are expressed in gray, and provided detailed structural information than those in color.

magnitude of the signal following excitation recovers as a function of T_1-, and the echo signal declines with that of T_2. The relationship between the repetition time (TR) and the echo time (TE) in the pulse sequences for MR images provide the relaxation time-weighted images. T_1-weighted images emphasize the area where a low mobility proton is present while T_2-weighted images emphasize the area where a high mobility proton is present. Additionally, T_2^*-weighted images represent the area dependent on homogeneity or susceptibility of the magnetic field and the molecular motions. In addition to relaxation time-weighted methods, chemical shift selective imaging allows for the acquisition of separate MR images for water and lipids, and then eliminates the overlapping signals of the water and lipids since the two signals are well-separated by their chemical shifts.

3.3. MR images with lipid suppression

In order to obtain MR images with only protons of water, all the MR images in Fig. 2D–F were acquired with lipid suppression, in addition to chemical shift selective images of water. When the images are compared with the T_1-weighted MR image without lipid suppression (Fig. 2A), it is clear that the signal intensity was reduced due to the loss of T_1 from mobile lipids of the soybeans (Fig. 2D). In addition, lipid signal was dominated in the T_2-weighted MR images as shown in Fig. 2C–F that are the images with and without lipid suppression, respectively, because T_2-relaxation time of the lipid is shorter than that of the water. The T_2^*-weighted MR images (Fig. 2B and D) show more detailed structural information as compared to other images due to the short echo time (TE) of 4.3 ms. Applying a magnetic field to a biological component generates an induced field characteristic of the specific tissue. The induced magnetization depends on the applied magnetic field, as well as on the magnetic susceptibility of the molecules (Hermier & Nighoghossian, 2004). The magnetic susceptibility varies at the interface of two regions, due to the generation of an intrinsic gradient, which is proportional to the difference in the magnetic susceptibility of the two adjoining structures (Liang et al., 1999). This T_2^*-weighted MR imaging enables the detection of acute hemorrhage (Schellinger,

Jansen, Fiebach, Hacke, & Sartor, 1999) and intravascular clots (Flacke et al., 2000) in clinical practice. There were slight differences in the signal intensity of the T_2^*-weighted MR images with and without lipid suppression, indicating the overlapping signals of the water and lipid not suppressed. Therefore, it was determined that all the relaxation time-weighted MR images originated from the water and lipid signals in the absence of lipid suppression, even with the chemical shift selective imaging.

3.4. Chemical shift artifacts in the measurement of water distribution by MR imaging

The MR images in Fig. 2A–C also show chemical shift artifacts which are from the superimposition of two MR images since there are two separate signals in the static ^{1}H NMR spectrum for the lipid and water; this is particularly noticeable when MRI experiments are performed at high magnetic fields (Wheeler, 1995). Chemical shift artifacts are generally classified as two separate effects: phase cancellation and shadow misregistration (Woodward, 2001). Phase cancellation results from the out-of-phase precession of the spins for water and lipid during the evolution of the free induction decay (FID) signal. The shadow misregistration of voxels (SM in 2) containing lipid occurs primarily in the frequency-encode direction (vertical in Fig. 2), and is due to the incorrect spatial mapping of voxel protons as a result of their different Larmor frequencies. Lipid suppression techniques, therefore, are often used to reduce these artifacts. The lipid suppression in chemical shift selective MR images in this study compensated for the chemical shift artifacts as shown in Fig. 2D–F. This indicates the chemical shift selective MR imaging of water is not enough to exclude the effects of other protons such as lipids; thus lipid suppression is essential for MR imaging in soybean seeds.

It was suggested in this study that the MR imaging of water should be performed by selecting the chemical shift of water and suppressing the lipid signal simultaneously, Also T_1-weighted images are more effective for investigating water distribution than T_2- and T_2^*-weighted images in soaked soybean seeds. The MR images of the peanuts soaked for 15 h were obtained using the same methods, as shown in Fig. 3. These images also show the chemical shift artifacts from the superimposition of the MR images

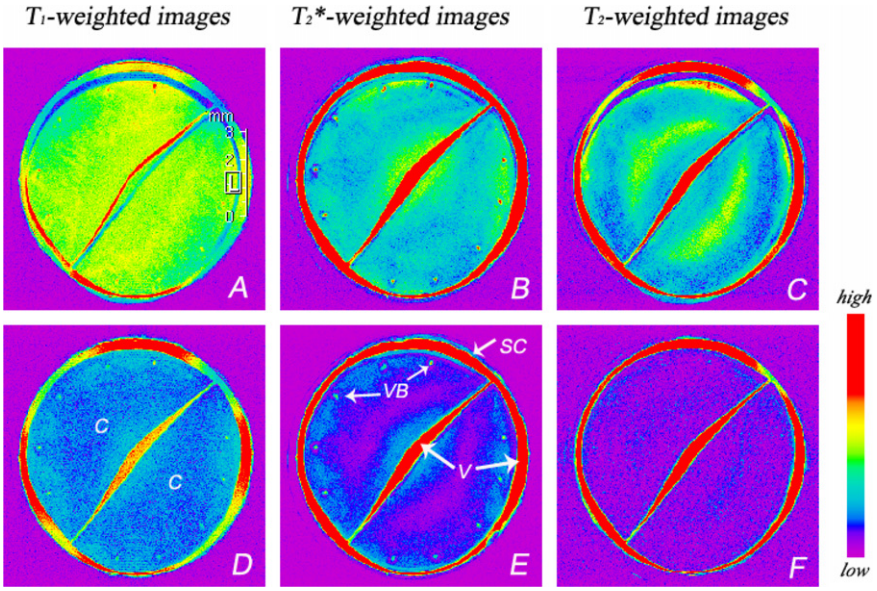

Fig. 3. Chemical shift selective MR images of water in peanuts soaked in water for 15hrs, using spin- and gradient echo sequences. A, B, and C are chemical shift selective T_1-, T_2^*-, and T_2-weighted MR images, respectively, without lipid suppression, and D, E, and F are chemical shift selective T_1-, T_2^*-, and T_2-weighted MR images, respectively, with lipid suppression. All images show central slices in the axial plane. The MR images were obtained with 35 × 35 μm^2 in-plane resolution and a 1 mm slice thickness. C, cotyledons; VB, vascular bundles; SC, seed coat and V, void between cotyledons or between seed coat and cotyledons.

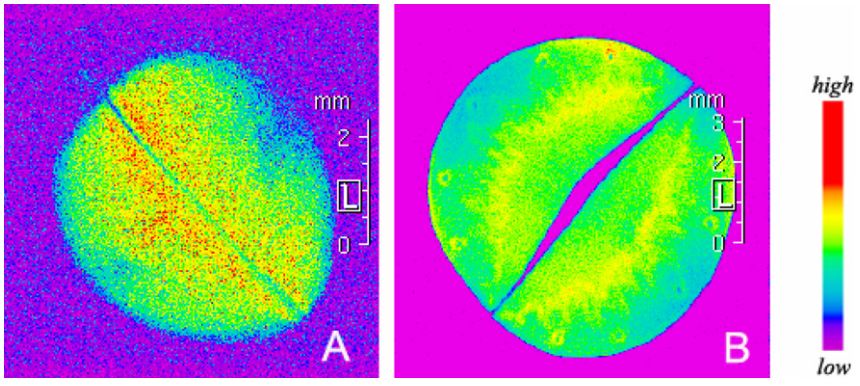

Fig. 4. Chemical shift selective T_1-weighted MR images of the lipid in seeds using MSME sequence with water suppression in soybeans (A) and peanuts (B) soaked in water for 15 h. All images show central slices in the axial plane. The MR images were obtained with 27 × 27 μm^2 (soybeans) and 35 × 35 μm^2 (peanuts) in-plane resolution, and with a 1 mm slice thickness.

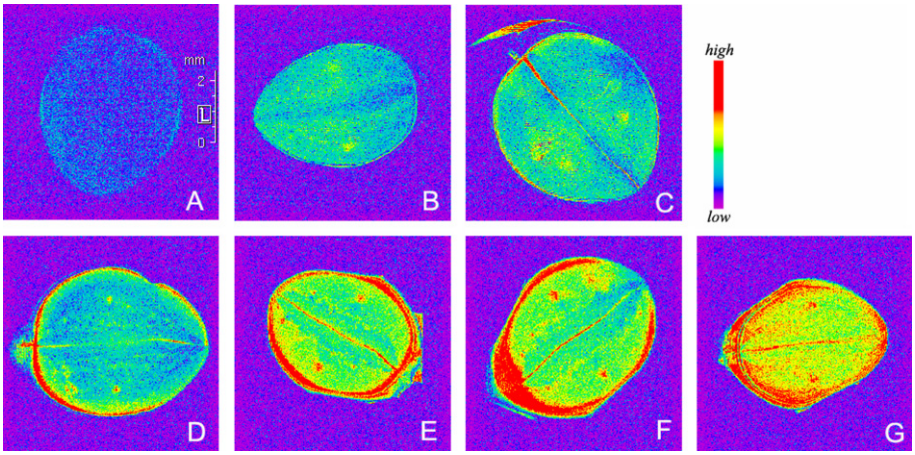

Fig. 5. Water distribution by chemical shift selective T_1-weighted MR images using the MSME sequence with lipid suppression, with increasing soaking and cooking times for the soybeans. A, B, and C are images of water in soybeans soaked in water for 1 h, 4 h, and 15 h, respectively. D, E, F, and G are images of water in soybeans cooked in water for 5 min, 30 min, 1 h, and 2 h, respectively. The MR images were obtained with 27×27 μm^2 in-plane resolution and a 1-mm slice thickness. TE and TR were 7.4 ms and 600 ms, respectively.

and the compensation for the artifacts, as well as the corrected water distribution. In addition to the chemical shift selective MR images of water with lipid suppression, the chemical shift selective MR images of lipid with water suppression were obtained in both the soybean and peanut seeds, as shown in Fig. 4. The highest signal intensity for lipid was found in the inner part of the cotyledons for both seeds. The lipid distributions in cotyledons have been also reported in mature soybean seeds (Borisjuk et al., 2005). The accumulation of lipids in the inner part of the cotyledons seemed to induce the magnetic susceptibility of the local regions, as shown in Fig. 2B and D, and Fig. 3B and D.

The superimposition of two signals, one from water and one from lipids, for the MR images of western white pine, was also reported (Terskikh et al., 2005). This research, however, only applied the chemical shift selective method to separate the MR images for oil and water. In addition, T_2-weighted MR images were acquired in pasta filata mozzarella cheese without using suppression or chemical shift selection methods (Kuo, Anderson, & Gunasekaran, 2003). If the MR images had been acquired using chemical shift selection and lipid or water suppression methods simultaneously, as well as relaxation time-weighting methods, corrected MR images would have been obtained, such as in the MR images of tempura and table olives (Brescia, Pugiese, Hardy, & Sacco, 2007; Horigane et al., 2003).

3.5. Water distribution during the soaking and cooking of soybeans

Fig. 5 shows the T_1-weighted MR images for water distribution in the soaked (A–C) and cooked soybean (D–G). The MR images were obtained using the MSME sequence with the chemical shift selection of water and simultaneous lipid suppression at 1, 4, and 15 h of soaking time. It was clear that the signal intensity of the water was increased with increasing soaking time, without contributions from the lipid signals, indicating an increase in water uptake, as shown in Fig. 5A–C. During cooking of the soybeans, the highest amount of water was found in the voids between the seed coats, and cotyledons, between cotyledons, and in the vascular bundles (VB). The lowest amount of water was found in the inner part of the cotyledons due to the presence of lipids, as described above.

4. Conclusions

This study was performed to understand water distribution by MR imaging in soaked and cooked soybean seeds. To obtain exact water distribution it is important to acquire MR images from the signal of water, excluding the lipid signal. The chemical shift selective T_1-, T_2^*-, and T_2-weighted MR images were composed of total proton signals, including both water and lipid signals, and showed chemical shift artifacts in the soaked soybean seeds. When the lipid suppression method was applied to the images the water images could be obtained independently, and compensated for the chemical shift artifacts. This study, therefore, demonstrates that the chemical shift selection of water with simultaneous lipid suppression, can offer MR images acquired with only a water signal and without any artifacts, in seeds containing high lipid content.

Acknowledgements

This study was partially supported by the Ministry of Health and Welfare (A050376) and the KOSEF (Korea Science and Engineering Foundation, # R01-2003-000-10717-0), and the Bio-MR Research Program (E27070) from the Korean Ministry of Science and Technology, Republic of Korea.

References

Agbo, G. N., Hosfield, G. L., Uebersax, M. A., & Klomparens, K. (1987). Seed microstructure and its relationship to water uptake in isogenic lines and a cultivar of dry beans (*Phaseolus* vulgaris L.). *Food Microstructure, 6*, 91–102.

AOAC, (1990). *Official Methods of Analysis*. Arlington: Association of Official Analytical Chemists.

Borisjuk, L., Nguyen, T. H., Neuberger, T., Rutten, T., Tschiersch, H., Claus, B., et al. (2005). Gradients of lipid storage, photosynthesis and plastid differentation in developing soybean seeds. *New Phytologist, 167*, 761–776.

Brescia, M. A., Pugiese, T., Hardy, E., & Sacco, A. (2007). Compositional and structural investigations of ripening of table olives, Bella della Daunia, by means of traditional and magnetic resonance imaging analyses. *Food Chemistry, 105*, 400–404.

Deshpande, S. S., & Cheryan, M. (1986). Microstructure and water uptake of Phaseolus and winged beans. *Journal of Food Science, 51*, 1218–1223.

Flacke, S., Urbach, H., Keller, E., Traber, F., Hartmann, A., et al. (2000). Middle cerebral artery (MCA) susceptibility sign at susceptibility-based perfusion MR imaging: Clinical importance and comparison with hyperdense MCA sign at CT. *Radiology, 215*, 476–482.

Glidewell, S. M. (2006). NMR imaging of developimg barely grains. *Journal of Cereal Science, 43*, 70–78.

Gruwel, L. H., Chatson, B., Yin, X. S., & Abrams, S. (2001). A magnetic resonance study of water uptake in whole barley kernels. *International Journal of Food Science and Technology, 36*, 161–168.

Hermier, M., & Nighoghossian, N. (2004). Contribution of susceptibility-weighted imaging to acute stroke assessment. *Stroke, 35*, 1989–1994.

Horigane, A. K., Motoi, H., Irie, K., & Yoshida, M. (2003). Obersevation of the structure, moisture distribution, and oil distribution in the coating of tempura by NMR micro imaging. *Journal of Food Science, 68*, 2034–2039.

Irie, K., Horigane, A. K., Naito, S., Motoi, H., & Yoshida, M. (2004). Moisture distribution and texture of various types of cooked spaghetti. *Cereal Chemistry, 81*, 350–355.

Kuo, M.-I., Anderson, M. E., & Gunasekaran, S. (2003). Determining effects of freezing on pasta filata and non-pasta filata mozzarella cheeses by nuclear magnetic resonance imaging. *Journal of Dairy Science, 86*, 2525–2536.

Lee, C. H. (2001). *Fermentation Technology in Korea. Seoul: Korea University Press.*

Liang, L., Korogi, Y., Sugahara, T., Shigematsu, Y., Okuda, T., Ikushima, I., et al. (1999). Detection of intracranial hemorrhage with susceptibility-weighted MR sequences. *American Journal of Neuroradiology, 20*, 1527–1534.

Manz, B., Muller, K., Kucera, B., Volke, F., & Leubner-Metzger, G. (2005). Water uptake and distribution in germinating tobacco seeds investigated in vivo by nuclear magnetic resonance imaging. *Plant Physiology, 138*, 1538–1551.

Marbach, T., & Mayer, A. M. (1974). Permeability of seed coats as related to drying conditions and metabolism of phenolics. *Plant Physiology, 54*, 817–820.

Mohoric, A., Vergeldt, F., Gerkema, E., de Jager, A., van Duynhoven, J., van Dalen, G., et al. (2004). Magnetic resonance imaging of single rice kernels during cooking. *Journal of Magnetic Resonance, 171*, 157–162.

Pietrzak, L. N., Fregeau-Reid, J., Chatson, B., & Blackwell, B. (2002). Observations on water distribution in soybean seed during hydration processes using nuclear magnetic resonance imaging. *Canadian Journal of Plant Science, 82*, 513–619.

Schellinger, P. D., Jansen, D., Fiebach, J. B., Hacke, W., & Sartor, S. (1999). A standardized MRI stroke protocol comparision with CT in hyperacute intracerebral hermorrhage. *Stroke, 30*, 765–768.

Schwartzberg, H. G., & Chao, R. Y. (1983). Solute diffusivities in leaching processes. *Food Technology, 36*, 75–98.

Terskikh, V. V., Feurtado, J. A., Ren, C., Abrams, S. R., & Kermode, A. R. (2005). Water uptake and oil distribution during imbibition of seeds of western white pine (Pinus monticola Dougl ex D. Don) monitored in vivo using magnetic resonance imaging.. *Planta, 221*, 17–27.

Vertucci, C. W. (1989). Seed moisture. In P. C. Stanwood & M. B. McDonald (Eds.), *The kinetics of seed imbibition: Controlling factors and relevance to seeding vigor* (pp. 93–115). Madison: Crop Science Society of America.

Wheeler, G. (1995). Articacts. In P. Woodward & R. D. Freimarck (Eds.), *NMR for technologists* (pp. 222–243). New York: McGraw-Hill.

Woodward, P. (2001). *MRI for technologists*. New York: McGraw-Hill.